

Influence of polymer swelling and dissolution into food simulants on the release of graphene nanoplates and carbon nanotubes from poly(lactic) acid and polypropylene composite films

Hristiana Velichkova, Ivanka Petrova, Stanislav Kotsilkov, Evgeni Ivanov, Nikolay K. Vitanov, Rumiana Kotsilkova

Institute of Mechanics, Bulgarian Academy of Sciences, Acad. G. Bonchev Street, Block 4, Sofia, Bulgaria

Correspondence to: R. Kotsilkova (E-mail: kotsilkova@imbm.bas.bg)

ABSTRACT: The study compared the effects of swelling and dissolution of a matrix polymer by food simulants on the release of graphene nanoplates (GNPs) and multiwall carbon nanotubes (MWCNTs) from poly(lactic) acid (PLA) and polypropylene (PP) composite films. The total migration was determined gravimetrically in the ethanol and acetic acid food simulants at different time and temperature conditions, while migrants were detected by laser diffraction analysis and transmission electron microscopy. Swelling, thermal analysis, and scanning electron microscopy were applied to characterize the degradation of polymer films at the migration conditions. The release of nanoparticles was found in a high-temperature migration test of 4 h at 90 °C. The hydrolytic dissolution of the PLA polymer in the food simulants caused a migration of GNPs (>100 nm) from the PLA/GNP/MWCNT films into the simulant solvents, while the entangled MWCNTs formed a network on the film surface, preventing their migration from the PLA composite films. In contrast, the PP polymer slightly swells in ethanol solvents, allowing some short carbon nanotubes to be released from the surface and cut edges of the PP/MWCNT film into food simulants. Mathematical modeling of diffusion was applied that accounts for type of polymer, time–temperature conditions, and solvent concentration; model parameters were validated with experimental results.

© 2017 Wiley Periodicals, Inc. *J. Appl. Polym. Sci.* **2017**, *134*, 45469.

KEYWORDS: biodegradable; degradation; packaging; swelling

Received 31 March 2017; accepted 27 June 2017

DOI: 10.1002/app.45469

INTRODUCTION

Researchers in food packaging technology are actively exploring the potential of polymer nanotechnology in order to answer the increased requirements for packaging materials to be stronger but lightweight, have certain functional properties, and increase the shelf life of the food.^{1,2} Incorporation of multiwall carbon nanotubes (MWCNTs) and graphene nanoplates (GNPs) in poly(lactic) acid (PLA) and polypropylene (PP) is a promising approach for food packaging applications, leading to several benefits, such as improved mechanical, thermal, and barrier properties of the polymeric films.^{2–5} It was recently found that carbon nanotubes and graphene have unique antimicrobial properties at direct contact with bacteria, due to electrostatic repulsion and oxidative stress.⁶ Such properties make graphene and carbon nanotubes attractive nanofillers for active, reinforced, and smart packaging materials in food applications.

Despite the many advantages of nanotechnology, there were serious uncertainties in the use of graphene and carbon nanotube-based composites as materials in contact with food

that were related to consumer exposure to those nanoparticles through migration into food and drink. Both graphene nanoplates and carbon nanotubes fall under the definition of nanomaterial according to (EU) No. 696/2011.⁷ The migration of substances into foodstuff is an important aspect of food packaging. Migration is a complex diffusion process from a theoretical point of view and is influenced by the concentration gradient of the additive, its solubility, the nature of the food simulant, temperature, and contact time.⁸ Some theoretical studies reported that nanoparticles larger than 3–4 nm in diameter cannot migrate (following a Fickian law of diffusion) from commodity plastics films, when fully incorporated in plastic film.^{9–11} It is generally believed that because of the fixed or embedded nature of nanoparticles in polymer, they will not migrate from film into food and thus not pose a risk to the consumer.¹²

The chemical stability of the matrix polymers in food simulant solvents is an important characteristic that has to be taken into account when analyzing the migration. The dissolution or degradation of the matrix polymer in the food simulant solvents

© 2017 Wiley Periodicals, Inc.

may assist the release of nanoparticles from the nanocomposite film into the surrounding media. Duncan *et al.*¹³ considered two routes for the release of nanoparticles from polymer films: via passive diffusion, desorption, and dissolution from the surface of the film into the liquid media; and via matrix degradation.¹⁴ Schmidt *et al.*¹⁵ found that asymmetric clay platelets of lateral size 50–800 nm indeed migrate from PLA composite film into food simulant (95% ethanol) due to matrix degradation. These authors observed the PLA polymer degradation by the shift of the molecular mass distribution of the polymer before and after migration contact.

The polymers of choice in this study are the biodegradable poly(lactic) acid (PLA) polymer produced from natural sources and the polypropylene (PP) that is an oil-based polymer; both are widely used for food packaging applications. Researchers have reported^{16–19} that ethanol and other polar solvents are aggressive to PLA polymer due to hydrolysis, leading to the release of lactic acid monomers, dimers, and oligomers. The PLA degradation products are subsequently hydrolyzed in aqueous systems to lactic acid, which is a natural product and food ingredient. In contrast, polypropylene is more resistant to organic chemicals than are most other commercially available thermoplastics.²⁰ In some studies, the swelling process was found to be dominant for polypropylene in the ethanol-based solvents.²¹ To our knowledge, no attempt has been made to characterize materials migrated from PLA and PP composite films incorporating graphene nanoplates and carbon nanotubes into food simulants. Moreover, it has not yet been explored in depth if the partial degradation of the matrix polymer by the food simulant solvents may cause a release of graphene nanoplates and carbon nanotubes from the plastic films.

The main objective of the present work is to report experimental data for overall migration from the composite PLA and PP films, incorporating 2 wt % carbon nanofillers (graphene nanoplates and carbon nanotubes), as well as to detect migration of GNPs and MWCNTs. The effect of high-temperature migration conditions on polymer degradation and the enhanced molecular mobility on overall migration are discussed. Neither graphene nanoplates nor carbon nanotubes are found in the list of materials explicitly authorized and included in the European Plastics Regulation specifications.^{22–24} The possible migration of graphene nanoplates and carbon nanotubes into food is of great concern because of their toxicity and similarity to asbestos, so they may cause adverse health and environmental effects.^{25,26} Therefore it is important to characterize migrants from nanocomposite films containing graphene and carbon nanotubes into different food simulants while varying the time–temperature migration conditions. Here the migrants in the food simulants were detected by laser diffraction analysis and high-resolution transmission electron microscopy. The degradation of the polymer before and after migration tests was investigated by swelling tests, thermal analysis, and scanning electron microscopy. Migration modeling was applied to predict the diffusion coefficient and concentration of migrants released from nanocomposite films depending on the matrix polymer, temperature, and solvent concentration.

EXPERIMENTAL

Materials

A thermoplastic masterbatch of graphene/poly(lactic) acid polymer containing 8 wt % graphene nanoplates and short multiwall carbon nanotubes (GRAPH-PLA) was supplied by Graphene 3D Lab, Calverton, NY, USA. The PLA4043D Ingeo Biopolymer, supplied by NatureWorks, Minnetonka, MN, USA, is synthesized from a family of lactic monomers with different molecular weights: L-100, L-300, L-800, and M-3000. The average molecular weight of the final PLA polymer is around MW \approx 160,000 DA. The residual lactide from the PLA pallets is reported to be <0.3% in total, where the residual D,L-lactide is <0.13% and the meso-lactide is <0.19%. Isotactic polypropylene (PP), Buplen 6231 (from Lukoil, Burgas, Bulgaria), and the commercial masterbatch Plasticyl PP2001 (from Nanocyl S.A., Sambreville, Belgium) containing 20% multiwall carbon nanotubes were used in this study.

Preparation of Nanocomposites and Films

The masterbatch of poly(lactic) acid nanocomposites with GNPs and MWCNTs was diluted with the neat PLA for production of the 2 wt % nanocomposites. Melt mixing in the temperature range 170–180 °C was applied. The 2 wt % MWCNT nanocomposite in polypropylene was prepared by dilution of the 20% PP/MWCNT masterbatch with neat PP in the temperature range 180–200 °C. Both nanocomposites were processed with a double-screw extruder at the screw speed of 45 rpm and then pelletized.

Films with thickness of \sim 30 μ m were fabricated by hot pressing of pellets at 190 °C. The nanocomposite films were named the PLA/GNP/MWCNT film and PP/MWCNT film, respectively. The neat PLA and neat PP films were prepared as control samples using the same pressing procedure as for the composite films. Test samples were cut from the films and subjected to further studies.

Swelling and Dissolution

The swelling behavior of the PLA-based and PP-based neat and composite films was investigated in three food simulants. Disk samples with diameter 3 cm and thickness 30 μ m were used for the swelling tests. The degree of swelling of the disk samples was determined gravimetrically by weighing the sample before the migration test, as well as the swollen sample after storage at the migration conditions studied. The excess dissolution medium was blotted out with tissue paper, and the samples were weighed in a high-precision analytical balance (\pm 0.01 mg). The disks were then dried to a constant weight in an oven at 37 °C. Each determination at each time point was performed in triplicate, and the standard deviation was calculated. The extent of swelling and dissolution occurring was considered. The degree of swelling (S , %) was calculated by the relative change of mass of the disk using eq. (1), similar to Kavanagh and Corrigan²⁷:

$$S = \frac{W_w - W_o}{W_o} \times 100\% \quad (1)$$

where W_w is the wet weight of the disk at a time t , and W_o is the initial weight of the disk.

The maximum measured degree of dissolution (D , %) occurring over the duration of the experiment was calculated for all compositions using eq. (2), by subtracting the dry weight of the disk from its wet weight and dividing this value by the dry weight at that time point²⁷:

$$D = \frac{W_w - W_d}{W_d} \times 100\% \quad (2)$$

where W_w is the wet weight of the disk at a time t , and W_d is the dry weight of the disk at the same time.

Migration Test

The testing conditions for evaluation of overall migration were taken from European Standard EN-1186-2002 with some modifications.²² Disk samples with diameter 3 cm, thickness 30 μm , and total surface area of 14 cm^2 were fully immersed in 30 mL of food simulant, and both sides were exposed to migration. Three aqueous food simulants were selected: 10% (v/v) ethanol (simulant A), 3% (v/v) acetic acid (simulant B), and 50% (v/v) ethanol (simulant D1), representing aqueous, acidic, and fatty foods, respectively.²³ The migration test was performed at two time-temperature conditions: 10 days at 40 °C (standard test), according to regulation EU 10/2011,²⁴ and 4 h at 90 °C (high-temperature test), aiming to mimic the migration of compounds from packaging films during microwaving, conventional heat treatment, and storage.¹⁹

Analysis of Total Migration

The overall migration from the polymeric films (mass of migrant per cm^2) in the three food simulants at two migration conditions (10 days at 40 °C and 4 h at 90 °C) was determined gravimetrically, using a modified standard procedure EN-1186-2002 for migration testing, proposed by Schmidt *et al.*¹⁵ After the contact time, the films were removed, and the simulant solvents were totally evaporated and dried in an oven at 105 °C for 30 min. The mass of the residue was determined with an analytical balance (± 0.01 mg accuracy) to determine the overall migration value of the simulant, as an average of three determinations (\pm standard deviation). A simulant blank was also measured. No volatile products in the total migrants are expected from the neat and the nanocomposite PLA and PP films that may be lost during the repeated heating, drying, and weighing cycle of the migration test method. This increases the reliability of the test method.

Laser Diffraction Analysis

The migrated simulant solvents were subjected to laser diffraction analysis to detect nanoscale migrants. The Analysette 22 Nano Tec plus (Fritsch, Idar-Oberstein, Germany) with a wet dispersion unit was used, having a detection limit of 0.020–2000 μm . A test sample of 10 mL of simulant solvent was added to 100 mL of distilled water and gently stirred during the test. The device allows the evaluation of the particle size distribution together with recognition of the particle shape in a single process. The result of the measurement was the average elongation calculated from the axis relation of an ellipsoid approximating the particles. The software provides a transformation of the equivalent volume-based data to number percentages. In our study, the measurements were performed within the range from 0.1 μm to 100 μm . The simulant blank solutions were also studied, and all total migration values are corrected for the blank value. The data for the

particle size distribution are presented as histograms of particle number percentage ($n\%$) versus particle size (μm).

Transmission Electron Microscopy

A high-resolution transmission electron microscope (TEMHR STEM JEOL JEM 2100, Peabody, MA, USA) at accelerating voltage 200 kV was used to analyze the dried colloids of migrated substances in the food simulants. A preliminary preparation technique for test samples was applied. A microquantity of colloid was dropped on a standard copper TEM grid covered by a membrane of amorphous carbon and was dried after that in a dust-free atmosphere at ambient conditions. TEM analysis was also applied to characterize the nanofiller dispersion in the composite films. Thin slides of about 80 nm from a cross section of the films were cut from the films and subjected to TEM visualization.

Scanning Electron Microscopy

Scanning electron microscopy (SEM) was used to visualize the morphology of the film surface before and after migration tests by using a digital Philips 515 microscope (North Billerica, MA, USA) with accelerating voltages 25 kV and 5 kV. Before the examination in the microscope, the samples were covered with a metal coating for better conductivity of the surface and to avoid discharge effects.

Thermal Analysis

A differential scanning calorimeter, DSC. Q20 (TA Instruments, New Castle, DE, USA) in nitrogen atmosphere was used to perform calorimetric analysis of the nanocomposite films before and after the migration tests. All test samples were accurately weighed into 100 μL aluminum pans to within 8.50 mg. The test was started by holding the samples at 30 °C for 5 min and then raising the temperature to 200 °C at 10 °C/min under nitrogen atmosphere. The samples were isothermally heated at 200 °C for 3 min and subsequently cooled back to 30 °C at -10 °C/min and held at that temperature for 3 min before heating again at 10 °C/min to 200 °C. The DSC characteristics were taken from the first and second heating cycles in order to see the influence of sample history. The glass-transition temperature (T_g), the crystallization temperature (T_c), and the melting temperature (T_m) were determined. The crystallinity ($\chi_c\%$) of the PLA polymer in the composite films before and after the migration tests was calculated from the DSC results by using the relation $\chi_c = (\Delta H_m / \Delta H_m^*) \times 100\%$, where ΔH_m is the melting enthalpy of PLA in the composite film, and ΔH_m^* is the melting enthalpy of pure crystalline PLA, having a value of 135 J/g, as suggested by Mitaya and Masuko.²⁸

RESULTS AND DISCUSSION

Characterization of Nanofiller Dispersion in Composite Films

TEM and SEM images of cross sections of the films are shown in Figure 1(a–c), visualizing the degree of dispersion of nanoparticles in PLA- and PP-based nanocomposite films. The TEM micrograph in Figure 1(a) for the composite PLA/GNP/MWCNT film shows a mixed nanofiller of graphene nanoplates with lateral sizes of nano- to microscale, as well as some short carbon nanotubes with length of ~ 500 nm, dispersed in between the graphene nanoplates. In Figure 1(b), the TEM micrograph of the composite PP/MWCNT film visualizes carbon nanotubes dispersed in smaller and larger agglomerates

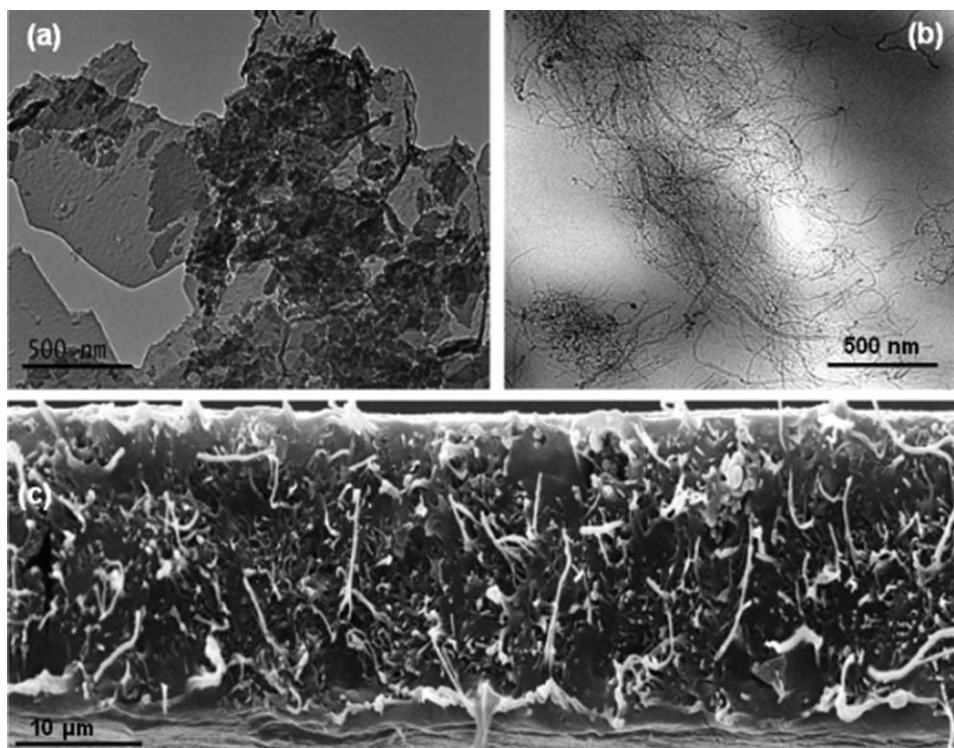


Figure 1. TEM and SEM visualization of the cross sections of composite films: (a,b) TEM micrographs of PLA/GNP/MWCNT and PP/MWCNT films, respectively, in magnification $\times 10,000$; and (c) SEM micrograph of the PLA/GNP/MWCNT film, in magnification $\times 1000$.

that form an entangled network in the PP matrix. As seen from the TEM analysis at magnification $\times 10,000$, the degree of nanofiller dispersion at the nanoscale was not perfectly homogeneous, but it consists of large and small agglomerates contacting each other. In contrast, at the microscale, the nanoparticles look to be homogeneously dispersed in the polymer, as shown in Figure 1(c) presenting the SEM micrograph of the cross section of PLA/GNP/MWCNT film at magnification $\times 1000$. Such a hierarchical structure of nanofiller in the polymer matrix is typical for polymer nanocomposites prepared by a top-down approach.

Migration Study

Total Migration. The total migration (mass of migrant per cm^2) was determined gravimetrically by drying the three food simulant solvents after the migration tests and weighing the residue. The results are summarized in Table I. Total migration was found for the neat PLA film and the composite PLA/GNP/MWCNT film after high-temperature migration conditions for 4 h at 90°C . Meanwhile, migration was not detected for the neat PP and the composite PP/MWCNT films at these high-temperature migration conditions, with the detection limit of ± 0.01 mg (accuracy of the analytical balance). We observed that the presence of carbon nanofiller in the PLA composite film increases the total migration (M_t) by 0.006 – 0.011 mg/cm^2 , if compared to the migration of the neat PLA films in the respective simulant solvent, which is assumed to be the approximate amount of nanofiller migrant (M_{NP}). The highest total migration ($M_t = 0.052$ mg/cm^2) that was observed for the composite PLA/GNP/MWCNT film in the acetic acid food simulant is two

times lower than the migration limit for overall migration (10 mg/dm^2) for food contact materials.^{22,24}

Swelling and Dissolution. The swelling of the neat PLA and PP films, as well as their composites PLA/GNP/MWCNT and PP/MWCNT, respectively, was estimated gravimetrically by weighing the film before and after storage in the food simulant solvents at two migration conditions. Swelling of the films was not observed during the standard migration test at 40°C for 10 days at the detection limit of ± 0.01 mg. Meanwhile, at the high-temperature migration conditions of 90°C for 4 h, a dissolution effect (decrease of mass, $D\%$) was found for the PLA-based films. The results are summarized in Table I. The dissolution of the PLA films in the food simulants might be indicative of partial hydrolytic degradation.¹⁹ Importantly, the nanocomposite PLA/GNP/MWCNT film showed a higher percentage of dissolution than that of the neat PLA film, due probably to the release of nanoparticle migrants. We assumed that the partial dissolution of the PLA polymer at the test conditions assisted the release of nanoparticles from the nanocomposite film into the simulant solvent. The nanoparticle migration was calculated by subtracting the value of neat PLA migrant from the value of the nanocomposite migrant. Thus, the approximate amount of nanoparticle migrant was 0.006 – 0.011 mg/cm^2 (Table I). If expressed in percentage, the released nanoparticles were about 0.14 – 0.25% from the incorporated amount of nanoparticles in the film.

In contrast, the neat PP polymer film was chemically stable in the three food simulant solvents at the high-temperature migration conditions. A slight swelling was observed only for the

Table I. Total Migrants and Degree of Swelling and Dissolution for Neat Polymeric Films and Composite Films into Food Simulants after Migration for 4 h at 90 °C

| Polymer type | Food simulant | Neat polymer film | | Nanocomposite film | | | Approximate nanofiller migrant M_{NP} (mg/cm ²) |
|-----------------|---------------------------|---|------------------------|---|------------------------|---------------------|---|
| | | Total migrant $M_{t,exp}$ (mg/cm ²) | Dissolution (D , %) | Total migrant $M_{t,exp}$ (mg/cm ²) | Dissolution (D , %) | Swelling (S , %) | |
| PLA-based films | 10% ethanol Simulant A | 0.022 ± 0.003 | 1.36 ± 0.012 | 0.028 ± 0.009 | 1.80 ± 0.019 | Not detected | 0.006 |
| | 3% acetic acid Simulant B | 0.042 ± 0.006 | 2.37 ± 0.010 | 0.053 ± 0.007 | 2.99 ± 0.025 | Not detected | 0.011 |
| | 50% ethanol Simulant D1 | 0.028 ± 0.005 | 1.65 ± 0.024 | 0.035 ± 0.004 | 1.95 ± 0.038 | Not detected | 0.007 |
| PP-based films | 10% ethanol Simulant A | Not detected | Not detected | Not detected | Not Detected | 0.18 ± 0.027 | Not detected |
| | 3% acetic acid Simulant B | Not detected | Not detected | Not detected | Not detected | Not Detected | Not detected |
| | 50% ethanol Simulant D1 | Not detected | Not detected | Not detected | Not detected | 0.30 ± 0.031 | Not detected |

nanocomposite PP/MWCNT films in 10% ethanol ($S = 0.18\%$) and 50% ethanol ($S = 0.30\%$) simulant solvents. Our results confirmed the Barson *et al.*²¹ reporting for swelling of PP into ethanol aqueous solvents of moderate concentrations.

Detection of Migrants in Simulant Solvents

Migrants from PLA-Based Films. Laser diffraction analysis was used to characterize the size distribution of the total migrants in the food simulant solvents. This instrumentation alone did not provide any information on the identity of nanoparticles and organic migrants occurring in the food simulant. To overcome this limitation, the laser diffraction analysis of the liquid solvents was combined with TEM analysis of the dried solvents. Importantly, migrants were not detected in the food simulants by TEM and laser diffraction analysis after the standard migration test of 10 days at 40 °C. Meanwhile, total migration was found after high-temperature migration tests for 4 h at 90 °C, particularly for the PLA-based films.

Figure 2(a–d) presents TEM micrographs of the total migrants detected in the dried food simulants, for the composite PLA/GNP/MWCNT film in the three food simulants: (a) 10% ethanol, (b) 50% ethanol, and (c,d) 3% acetic acid. In the insets, the size distribution histograms of migrants are compared for the neat PLA (dark bars) and the composite PLA/GNP/MWCNT films (light bars) in the three food simulant solvents.

The TEM micrographs in Figure 2(a–c) show that few layer graphene nanoplates of size around 100–1000 nm were able to migrate from the PLA/GNP/MWCNT in the three food simulants. While, carbon nanotubes fixed with organic substances were rarely detected to migrate in large agglomerates ($>2 \mu\text{m}$); this was observed mainly in the 3% acetic acid food simulant, which was more aggressive for the PLA polymer [Figure 2(d)]. The results from the laser diffraction analysis [insets in Figure 2(a–c)] demonstrate differences between the neat PLA film and the composite PLA/GNP/MWCNT film with respect to the particle size distribution of migrants in the corresponding solvents.

The PLA histograms (dark bars) show a bimodal size distribution with a small peak within the micrometer size range of 1–10 μm (0.3–1 $n\%$) and the main peak above 10 μm (9–12 $n\%$). The migrants obtained from the neat PLA film refer to the low-molecular-weight organic substances dissolved from the PLA matrix due to hydrolysis of the polymer chains.¹⁹ The histogram for the composite PLA/GNP/MWCNT film (light bars) shows the presence of migrants in nanoform (0.1–1 μm) that appeared in small amounts, $\sim 0.2 n\%$, in 50% ethanol and 3% acetic acid solvents. Such migrants were not found from the neat PLA film in the respective food simulants. Thus, the nano-scale migrants from the composite PLA/GNP/MWCNT films are associated with the released graphene nanoplates visible in the TEM micrographs. Moreover, the peak within 1–10 μm was much higher for the composite PLA/GNP/MWCNT film (1–4 $n\%$) compared to the neat PLA (0.3–1 $n\%$). The organic substances that migrated from the PLA polymer are detectable by the laser diffraction analysis, but due to their transparency they were not visible in the TEM micrographs.

Based on these results, we assume that the release of GNPs from the composite PLA/GNP/MWCNT film was caused by the partial polymer dissolution (hydrolysis) of PLA polymer in aqueous food simulants at the high-temperature migration conditions, mainly in 3% acetic acid and 50% ethanol. This led to a diffusion of graphene nanoplates together with the decomposed polymer chains from the film surfaces to the food simulants. The entangled MWCNTs released rarely in the aggressive acetic acid food simulant were preferably fixed with the dissolved organic matrix. This confirmed that the release of both nanofillers also depended on their compatibility with the matrix polymers in addition to polymer swelling and hydrolysis.

Migrants from PP-Based Films. Migrants from the composite PP/MWCNT films were rarely detected at the high-temperature migration conditions of 4 h at 90 °C. The TEM micrographs in Figure 3(a–c) visualize the migrants from the composite

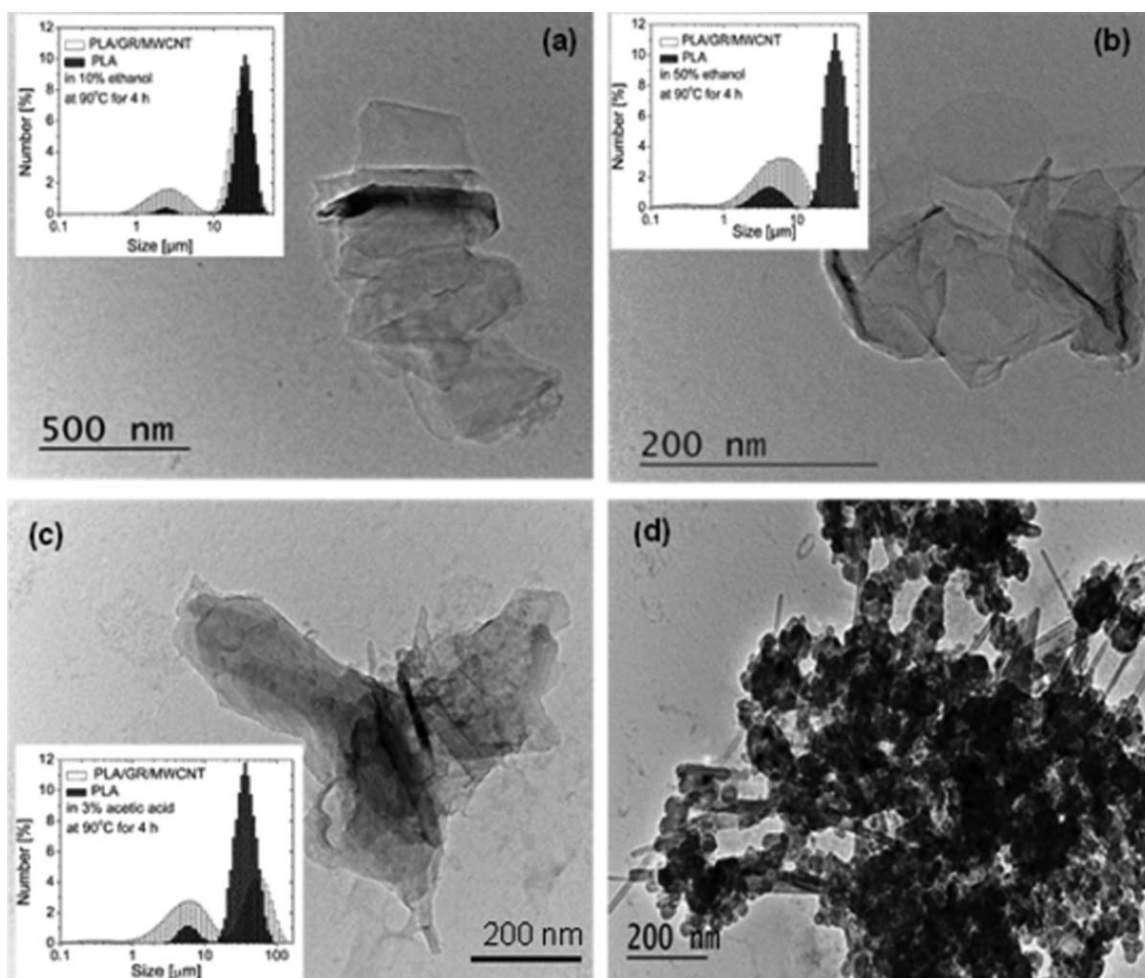


Figure 2. TEM micrographs of dried migrants from PLA/GNP/MWCNT film after high-temperature migration test (at 90°C for 4 h): (a) in 10% ethanol; (b) in 50% ethanol; (c,d) in 3% acetic acid. Insets: size distribution histograms of migrants from the neat PLA (dark bars) and PLA/GNP/MWCNT films (light bars) in the liquid food simulants.

PP/MWCNT film into 10% ethanol, 50% ethanol, and 3% acetic acid, respectively. Figure 3(d–f) compares the size distribution histograms of migrants from the neat PP (dark bars) and the composite PP/MWCNT films (light bars). Total migration from the neat PP films was found to be insignificant in the three food simulants. Migrants in nanoform of size 0.1–1 μm were observed in small amounts around 0.5 n% for the composite PP/MWCNT films in the ethanol-based food simulants [Figure 3(d,e)]. We associated the small amounts of nanoscale migrants with single, short carbon nanotubes of length above 100–200 nm and their aggregates, visible from the TEM micrographs in Figure 3(a,b). Meanwhile, carbon nanotube migrants were not observed in the acetic acid solvent, due probably to the insufficient swelling of the PP-based films during the migration test in this food simulant [Figure 3(f)].

It might be assumed that the swelling of the PP matrix in the ethanol-based solvents and the increased molecular mobility at high-temperature migration conditions assisted the release of the short carbon nanotubes that were weakly fixed with polymer at the surfaces and cut edges of the film. Our results complement that of Huang *et al.*²⁹ associating the diffusion of

migrants from a polymer film at high-temperature migration conditions with an increase of the total permeation flux, due to the higher flexibility of polymer chains above the glass transition, which caused a larger available free volume of polymer matrix for diffusion.

Characterization of the Films Affected by the Migration Tests
Microstructure of the Film Surfaces. SEM analysis was performed to characterize the microstructure of the PLA/GNP/MWCNT composite on the film surface and the cross section [Figure 4(a–f)] after the high-temperature migration test at 90°C for 4 h in the three simulant solvents. The control film before the migration test in Figure 4(a) shows a smooth surface without nanoparticles on it. After the migration test in 10% ethanol [Figure 4(b)], a small number of graphene nanoplates were migrated onto the film surface. In contrast, after migration in 50% ethanol [Figure 4(c)], the film surface became rich with graphene nanoplates, and a local surface-erosion process was observed. In Figure 4(d), an extraction of substances from the volume to the film surfaces was observed in 3% acetic acid, due probably to the partial PLA polymer degradation in this food simulant. The cross sections of the film after migration in 50%

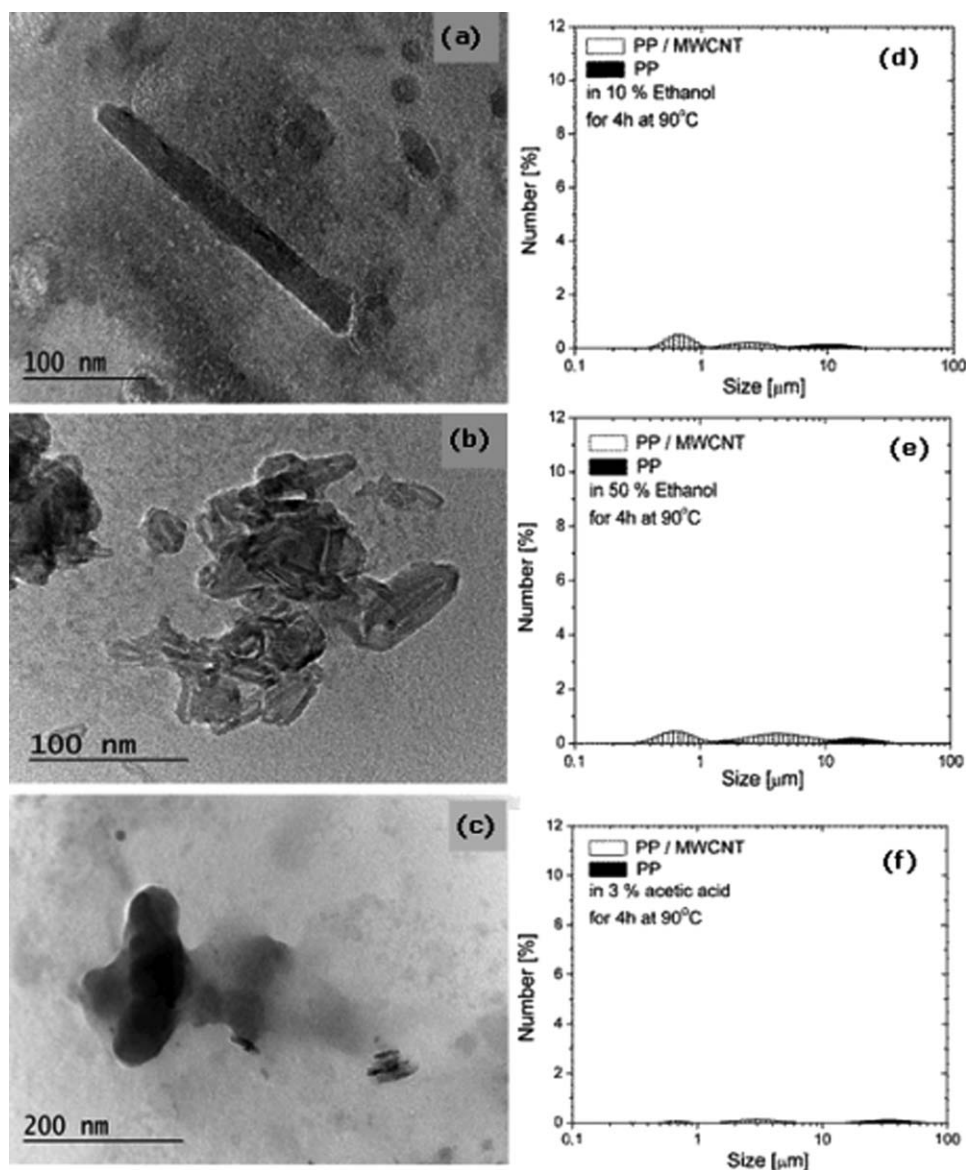


Figure 3. TEM micrographs of migrants from composite PP/MWCNT film detected in dried food simulants; and (d–f) size distribution histograms of migrants in the food simulant solvents after high-temperature migration tests in (a) 10% ethanol, (b) 50% ethanol, and (d) 3% acetic acid. The neat PP is represented by dark bars and the PP/MWCNT films by light bars.

ethanol [Figure 4(e)] and in 3% acetic acid [Figure 4(f)] also visualize the migration of substances at the cut ends of the composite films. Our results confirm the findings of Rodriguez *et al.*,³⁰ who reported on a hydrolytic degradation of PLA in acidic media due to autocatalysis, as determined by a decreasing molecular weight followed by a rapid weight loss.

Figure 5(a–d) presents the SEM micrographs of the PP/MWCNT film surfaces after the high-temperature migration test at 90 °C for 4 h in the three simulant solvents. The micrograph of the control composite film before the migration test [Figure 5(a)] shows that carbon nanotubes fixed with polymer were visible on film surfaces. Such movement of the MWCNTs to the polymer–air interface appeared during hot pressing of the film sample. It was observed that after the migration test of the composite film in the ethanol-based solvents [Figure 5(b,c)],

the carbon nanotubes became hidden in the polymer matrix. However, after the migration test in 3% acetic acid [Figure 5(d)], the carbon nanotubes were partly visible on the film surfaces. A significant extraction of organic substances from the volume to the film surface at the high-temperature migration conditions was not observed.

Characterization of Polymer Degradation. Calorimetric analysis was performed in order to characterize the influence of hydrolytic degradation of PLA polymer in the composite films during the high-temperature migration test at 90 °C for 4 h in the three food simulants. Figure 6(a,b) shows the DSC thermograms (first and second runs) of the PLA/GNP/MWCNT film and Figure 6(c,d) for the PP/MWCNT film (first run and cooling), before and after migration tests into the three food simulants.

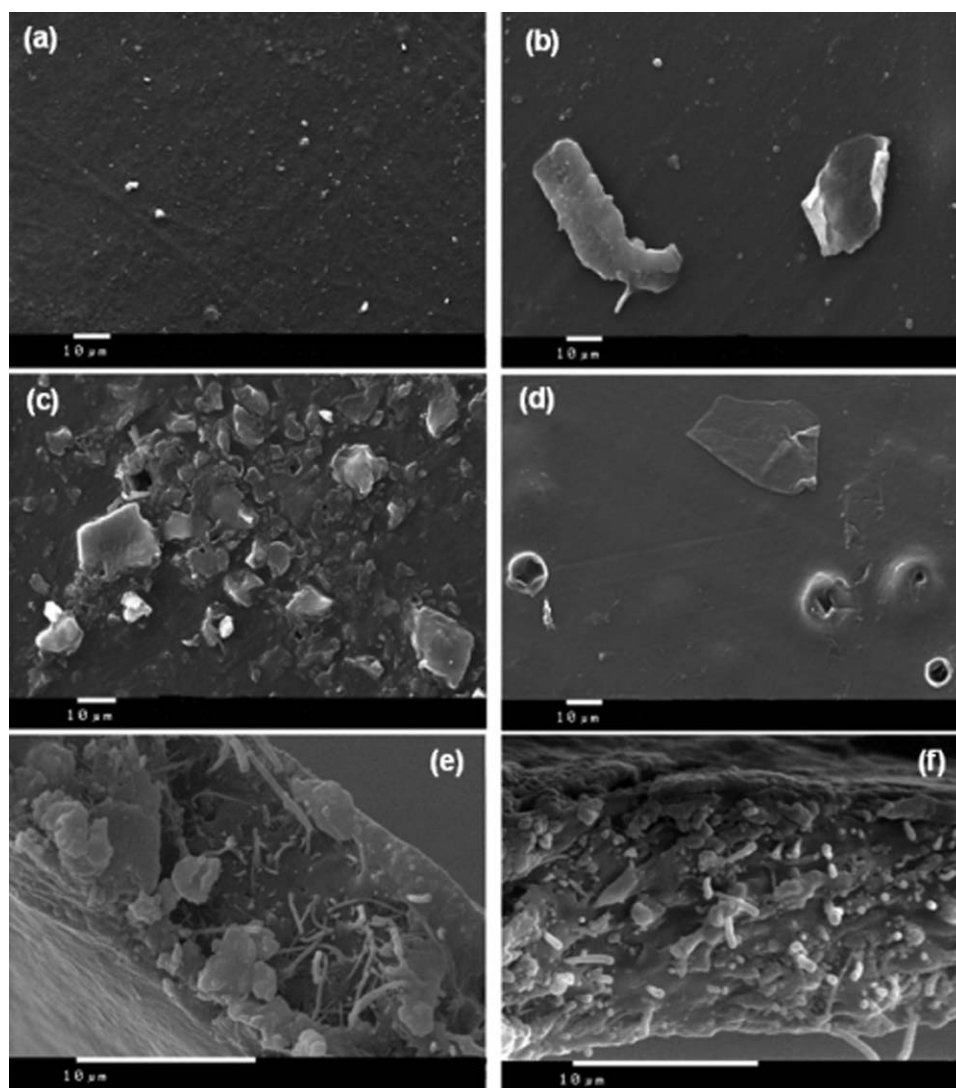


Figure 4. SEM micrographs of the surface of PLA/GNP/MWCNT film: (a) control film before migration test and after high-temperature migration test in (b) 10% ethanol, (c) 50% ethanol, and (d) 3% acetic acid, at magnification $\times 1000$; (e,f) SEM images of the cross section at the cut ends of composite films after migration in 50% ethanol and 3% acetic acid, at magnification $\times 5000$.

As shown in Figure 6(a), the peak ascribed to crystallization of the PLA polymer in the composite film was strong for the control film, but it did not appear for the migrated films during the first-run heating cycle. However, in the reheating second-run cycle [Figure 6(b)], a crystallization peak was observed for all films, but for the migrated films the peaks were not so strong, and the crystallization temperature (T_c) was shifted toward higher temperatures compared to the control film. Such changes of the crystallization peak imply that the crystallinity of PLA in the migrated composite films was slightly reduced during immersion in the simulant solvents due to hydrolysis at high temperatures. The change of crystallinity (χ_c) and fusion enthalpies (ΔH_m) due to hydrolysis of PLA were also examined. The crystallinity decreased from 5.6% for the control film to 4.0, 3.4, and 3.2% for the migrated films, while the enthalpies of fusion of PLA decreased from 7.5 for the control to 5.7, 4.6, and 4.3 J/g for the migrated films in 10% ethanol, 50% ethanol,

and 3% acetic acid, respectively. Obviously, hydrolysis of the semicrystalline PLA starts in the crystalline region, transforming these domains into amorphous phases,³¹ and the largest transformation was achieved in the acetic acid solvent, followed by the 50% ethanol food simulant.

The intensities of the melting peaks in Figure 6(a) also decreased slightly for the migrated composite films, and the melting temperature (T_m) is slightly shifted toward higher temperatures by about 2 °C, compared with the control film. Two melting peaks were observed in all of the PLA composite films that are not typical for the neat PLA, and they might be associated with the melting of the bond polymer at the polymer-nanofiller interfaces. A small increase of the glass-transition temperature (T_g) of 2–3 °C was observed in the first heating run for the films that were migrated in the ethanol simulants. The increase in the glass-transition (T_g) and melting temperatures of

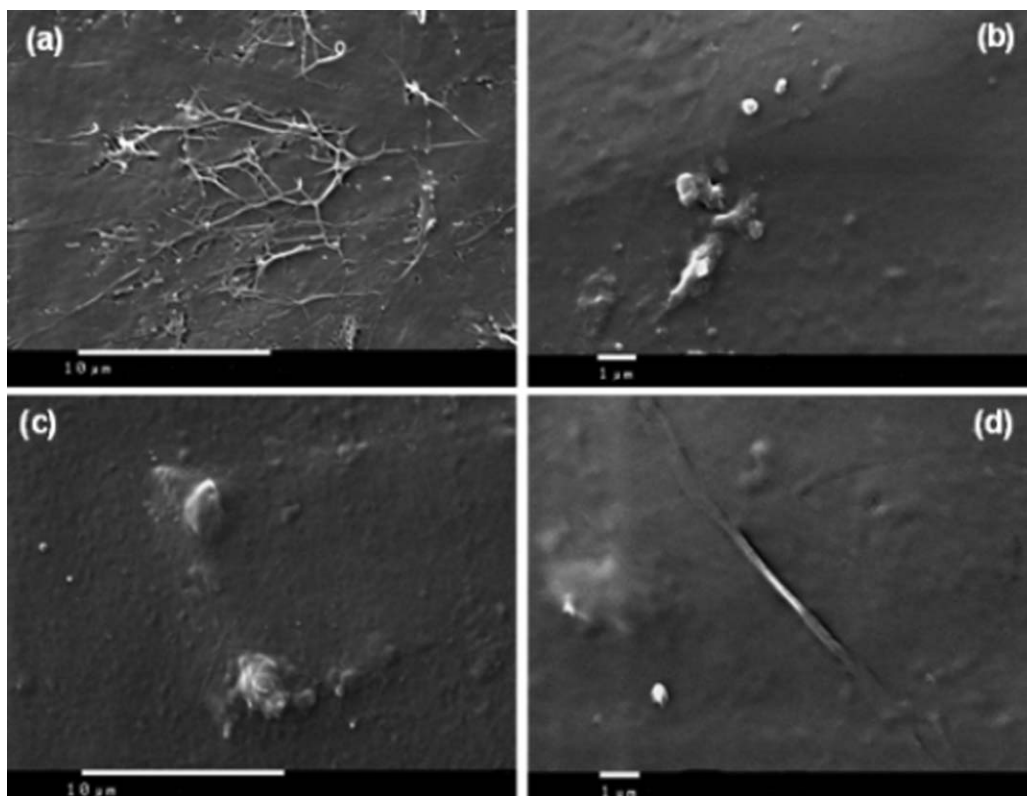


Figure 5. SEM micrographs of PP/MWCNT films after high-temperature migration tests for 4 h at 90 °C into three food simulants: (a) control film, (b) 10% ethanol, (c) 50% ethanol, and (d) 3% acetic acid, at magnification $\times 5000$ (a,c) and $\times 10,000$ (b,d).

the migrated films compared to the control film could be associated with minor changes in the polymer that influenced a slight increase of its high-molecular-weight fractions.³¹

Figure 6(c,d) shows DSC thermograms of the PP/MWCNT film in (a) the first heating run and (b) in the cooling regime in the crystallization peak temperature zone, comparing the control film and migrated films in the three food simulants. The thermogram for the second heating run is similar to that obtained from the first run, so it was not presented here. As seen from Figure 6(c), the melting temperature (T_m) was slightly shifted by 1–2 °C toward higher temperatures only for the films migrated in the ethanol simulants compared to the control film. The crystallization temperature (T_c) and the degree of crystallinity ($\chi\%$), determined from the cooling curve in Figure 6(d), were not affected by the simulant solvents after the high-temperature migration test. These results indicated that the time–temperature structural changes were insignificant for the PP/MWCNT films immersed in the three food simulants during the course of the migration test. The small shift of melting temperature T_m for the composite films migrated in ethanol-based simulants indicated the swelling of the PP polymer in the ethanol solvents.

Migration Modeling

Polymer dissolution in solvents usually leads to the diffusion of degraded polymer chains through a polymer–solvent interface layer, which is associated with migration.³² Our experimental results indicated that the partial degradation of PLA polymer due to hydrolytic dissolution by food simulants at high-

temperature migration conditions facilitated the migration of graphene nanoplates from the composite films. Thus the GNPs and the dissolved PLA organic substances diffused from the volume toward the film surface and then into the food simulants. Moreover, the type of penetrating food simulant solvent also had an effect on the PLA polymer dissolution.

When the polymer is not dissolved in the food simulant solvent, diffusion of a migrant from the polymer into the solvent can be described by the Fick diffusion equation using the diffusion coefficient^{33,34}:

$$\frac{\partial C}{\partial t} = D \frac{\partial^2 C}{\partial x^2} \quad (3)$$

where c is the amount of migrant in the polymer film at the time t (s), D is the diffusion coefficient of migrant within the polymer, and x is the position of the migrant along the thickness of the polymer film.

Recently, an empirical relationship between diffusion coefficient, molecular weight of migrant, and temperature was established for a range of engineering plastics (Brandsch *et al.*³⁵). Equation (4) was proposed, which is applicable to migrants of molecular weight in the range 100–2000 g/mol and represents an Arrhenius-like relationship³⁶:

$$D_p = 10^4 \exp \left[A_p - 0.1351 M_r^{\frac{2}{3}} + 0.003 M_r - \frac{10,454 R}{RT} \right] \text{cm}^2/\text{s} \quad (4)$$

where $A_p = A'_p - \tau/T$, M_r is the relative molecular mass of migrant, A'_p and τ are specific parameters of the polymer

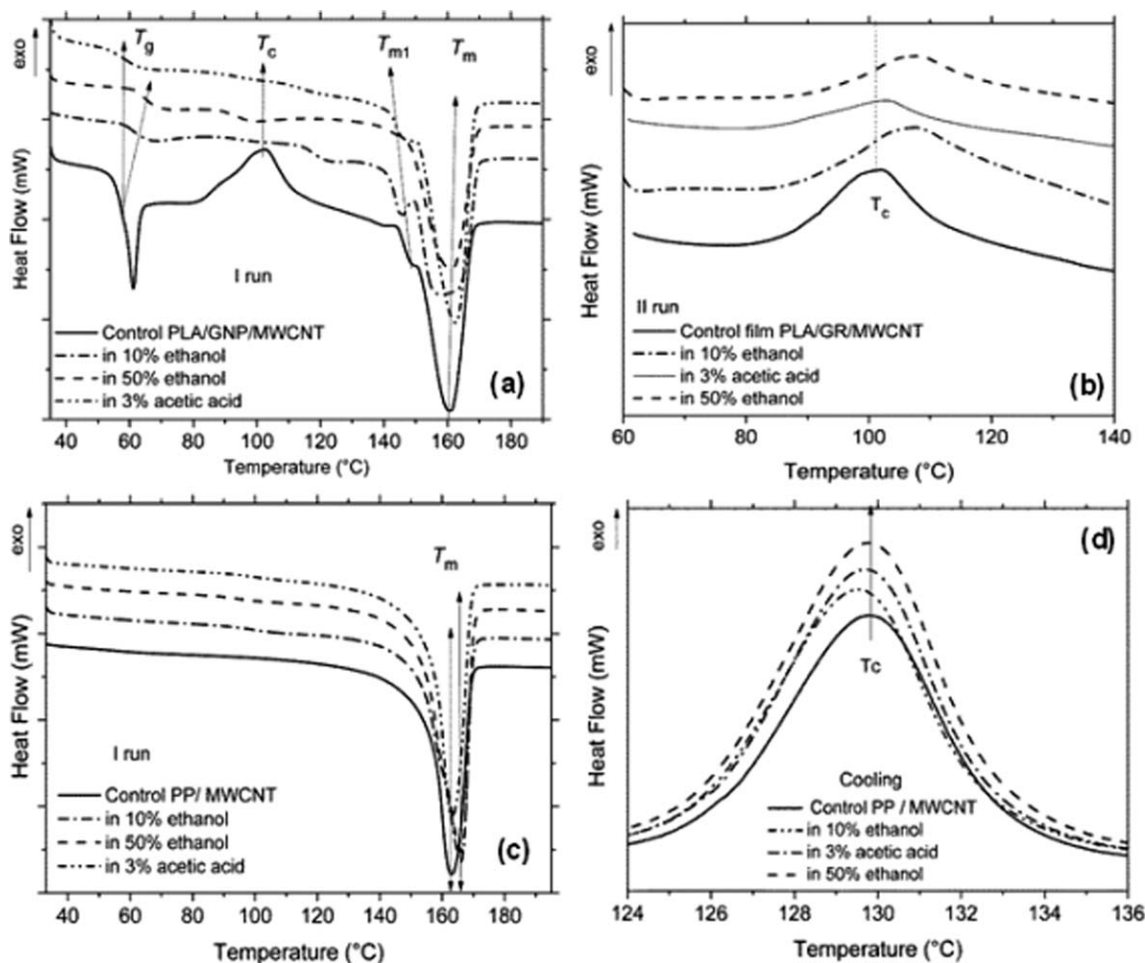


Figure 6. DSC thermograms of heat flow versus temperature: (a,b) first and second runs for PLA/GNP/MWCNT; (c,d) first run and cooling for the PP/MWCNT films, before and after migration tests in the three simulant solvents: 10% ethanol, 3% acetic acid, and 50% ethanol.

matrix, T is temperature (K), and $R = 8.3145$ (J/mol K) is the gas constant.

However, if the solubility of the polymer increased, a considerable amount of solvent was absorbed into the polymer. Due to swelling of the polymer, the diffusion rates of the solvent and the migrant were increased, and deviations from the model [eq. (3)] arise. The diffusion of compounds dissolved at the interface between the polymer and the solvent is often described by an empirical equation relating the diffusion coefficient with the solvent concentration³⁷:

$$D_F = D_P \exp(\gamma c_F) \quad (5)$$

where D_P (cm²/s) is the diffusion coefficient of migrant in the polymer at zero solvent concentration, c_F (mg/cm³) is the concentration of food simulant solvent, and γ is an adjustable parameter.

The total amount (M_t) of diffusing substance that left the film at time t is given by the simplified equation $M_t = 2M_0 (Dt/\pi)^{1/2}$ (from Crank³⁸). We used the simplified form for migrants from the two sides of the thin planar polymer film immersed in a large volume of food simulant solvent.³⁹ The concentration of migrant at the boundary condition, $x=L$, that

is, at the “polymer film surface,” was determined by eq. (6) by introducing an error function $\Phi(z)$, calculated from $\Phi(z) = (2/\sqrt{\pi}) \int_0^z d\mu \exp(-\mu^2)$, assuming that $\mu = (x-)/(2\sqrt{Dt})$ and $\mu = (x+)/(2\sqrt{Dt})$:

$$M_t = 4 \frac{M_0}{L} \Phi \sqrt{\frac{D_F t}{\pi}} \quad (6)$$

where M_t (mg/cm²) is the total amount of diffusion substance that has entered the food simulant medium at time t (s), M_0 (mg/cm³) is the initial concentration of migrant in the polymer film, L (cm) is the thickness of the film, D_F (cm²/s) is the diffusion coefficient dependent on the solvent concentration, and Φ is the error function.

In our study, migration modeling was applied to the neat PLA and the composite PLA/GNP/MWCNT films, where total migrants of degraded polymer molecules and graphene nanoplates were detected to release from the films into the food simulants. In the calculations, the key modeling parameters in eq. (3) for the PLA polymer were taken as equal to those of polyesters (above T_g), and thus $M_r \sim 800$ g/mol (the molecular weight for lactic acid dimers, to oligomers varying from 306 to 1200 g/mol), $A_p = 6.4$, $\tau = 1577$, and $T = 363$ K (the

Table II. Estimated Diffusion Modeling Parameters of the Neat PLA and Composite PLA/GNP/MWCNT Films Compared to Experimental Results for Simulant Solvents after Migration for 4 h at 90 °C

| Parameter | 3% Acetic acid | 10% Ethanol | 50% Ethanol |
|------------------------------------|------------------------|------------------------|------------------------|
| Neat PLA film | | | |
| D_P (cm ² /s) | 2.35×10^{-13} | 2.35×10^{-13} | 2.35×10^{-13} |
| D_F (cm ² /s) | 8.71×10^{-13} | 2.60×10^{-13} | 3.87×10^{-13} |
| M_o (mg/cm ³) | 100 | 100 | 100 |
| M_t (mg/cm ²) | 0.042 | 0.023 | 0.028 |
| $M_{t,exp}$ (mg/cm ²) | 0.042 ± 0.006 | 0.022 ± 0.003 | 0.028 ± 0.005 |
| PLA/GR/MWCNT | | | |
| D_P (cm ² /s) | 2.35×10^{-13} | 2.35×10^{-13} | 2.35×10^{-13} |
| D_F (cm ² /s) | 8.71×10^{-13} | 2.60×10^{-13} | 3.87×10^{-13} |
| $M_{o,NP}$ (mg/cm ³) | 24 | 24 | 24 |
| M_t (mg/cm ²) | 0.052 | 0.029 | 0.035 |
| M_{NP} (mg/cm ²) | 0.010 | 0.006 | 0.007 |
| $M_{t,exp}$ (mg/cm ²) | 0.053 ± 0.007 | 0.028 ± 0.009 | 0.035 ± 0.004 |
| $M_{NP,exp}$ (mg/cm ²) | 0.011 | 0.006 | 0.007 |

temperature of the migration test). In eq. (5), the concentration of food simulant solvents c_F was determined as 0.03, 0.1, and 0.5 for the 3% acetic acid and 10% and 50% ethanol simulant solvents, respectively, while $\gamma = 1$ and 3.6 are the values for the ethanol and the acetic acid solvents, respectively.⁴⁰ For the calculations in eq. (5), the initial amount of organic migrant $M_o \approx 100$ mg/cm³ (corresponding to ~ 8 wt %, which was the concentration of the soluble molecular weight in the neat PLA polymer, according to Crank³⁸), and $M_{o,NP} = 24$ mg/cm³ (corresponding to 2 wt % initial concentration of carbon nanofiller in the PLA/GNP/MWCNT composite). The error function in eq. (6), $\Phi = 0.005$, was determined at $z = 1$ and $\mu = 0.01$.

Table II presents the diffusion coefficients D_P and D_F (depending on the concentration and type of solvent) calculated using eqs. (4) and (5), as well as the amount of total migrants M_t and the nanoparticle migrant M_{NP} , calculated with eq. (6).

The modeling results demonstrate a very good correlation between the predicted amounts of total migrant M_t (0.023–0.042 mg/cm²) for the PLA-based films and the nanoparticle migrant M_{NP} (0.006–0.010 mg/cm²) for the composite PLA/GNP/MWCNT films (Table II), compared with the experimentally determined values for migrants.

CONCLUSIONS

The results from this study demonstrate that the swelling and partial hydrolytic dissolution of PLA polymer in ethanol and acetic acid food simulants caused the release of graphene nanoplates (100–1000 nm) from the composite PLA/GNP/MWCNT film at the high-temperature migration conditions of 90 °C for 4 h. The fibrous MWCNTs formed an entangled network in the PLA matrix, which prevented their release from the film surfaces when the PLA matrix dissolved. Hence, small amounts of MWCNTs fixed with the organic PLA rarely release as migrants in the most aggressive acetic acid food simulant. In general, the total amounts of migrants observed to release from the

composite PLA/GNP/MWCNT films were in the range of 0.028–0.053 mg/cm², which is much lower than the overall migration limit for food contact material (0.10 mg/cm²). In contrast, only a few short carbon nanotubes (100–200 nm in length) were detected to release from the surfaces and cut edges of the chemically stable PP/MWCNT composite film in 10 v/v % and 50 v/v % aqueous ethanol solvents. This was associated with the increased dynamics of PP polymer molecules in the high-temperature migration conditions, leading to a slight swelling, especially in ethanol-based food simulants. The migrated amount of MWCNTs was insignificant.

Mathematical modeling of diffusion was applied, where the diffusivity of migrant from the film toward the solvent media was modeled depending on the type of polymer, time–temperature conditions, and solvent concentration. The predicted amounts of migrants were found to be similar to the experimentally detected values.

ACKNOWLEDGMENTS

This research was supported by the H2020MSCA-RISE-734164 Graphene 3D and the H2020-604391-GRAPHENE-Core1 projects. Support from the Bulgarian “Science Fund” for the cofinanced project for COST CA15114-AMICI is acknowledged. The authors thank S. Gyoshev and N. Stoimenov from ICT-BAS for the laser diffraction measurements.

REFERENCES

- Silvestre, C.; Pezzuto, M.; Cimmino, S.; Duraccio, D. In *Eco-sustainable Polymer Nanomaterials for Food Packaging: Innovative Solutions, Characterization Needs, Safety and Environmental Issues*; Silvestre, C., Cimmino, S., Eds.; Taylor & Francis: UK, 2013; Chapter 1, pp 1–26.
- Wei, H.; Yan Jun, Y.; Ning Tao, L.; Li Bing, W. *J. Mater. Sci.* 2011, 56, 1216.

3. Ivanov, E.; Kotsilkova, R. In *Handbook of Nanoceramic and Nanocomposite Coatings and Materials*; Abdel Makhlof, A., Scharnweber, D., Eds.; Elsevier, Kidlington Oxford, UK, **2015**; Chapter 17, pp 351–383.
4. Wu, L. L.; Wang, J.; He, X.; Zhang, T.; Sun, H. *Packag. Technol. Sci.* **2014**, *27*, 693.
5. Brody, A. L.; Bugusu, B.; Han, J. H.; Sand, C. K.; Mchugh, T. H. *J. Food Sci.* **2008**, *73*, 8, 107.
6. Kang, S.; Herzberg, M.; Rodrigues, D. F.; Elimelech, M. *Langmuir* **2008**, *23*, 13, 6409.
7. European Commission Recommendation (EU 2011) of 18.10.2011 on the Definition of a Nanomaterial 2011/696/EU.
8. Bhunia, K.; Sablani, S. S.; Tang, J.; Rasco, B. *Compr. Rev. Food Sci. Food Saf.* **2013**, *12*, 5, 23.
9. Bott, J.; Stoermer, A.; Franz, R. *Food Packag. Shelf Life* **2014**, *2*, 73.
10. Simon, P.; Chaudhry, Q.; Bakos, D. *J. Food Nutr. Res.* **2008**, *47*, 3, 105.
11. Lin, Q. B.; Li, H.; Zhong, H. N.; Zhao, Q.; Xiao, D. H.; Wang, Z. W. *Food Addit. Contam. Part A* **2014**, *31*, 1284.
12. Chaudhry, Q.; Scotter, M.; Blackburn, J.; Ross, B.; Boxall, A.; Castle, L.; Aitken, R.; Watkins, R. *Food Addit. Contam.* **2008**, *25*, 241.
13. Duncan, T. V.; Pillai, K. *ACS Appl. Mater. Interfaces* **2015**, *7*, 2.
14. Duncan, T. V. *ACS Appl. Mater. Interface* **2015**, *7*, 20.
15. Schmidt, B.; Petersen, J. H.; Koch, C. B.; Plackett, D.; Johansen, N.; Katiyar, V.; Larsen, E. *Food Addit. Contam. Part A* **2011**, *28*, 956.
16. Lalanne, A.; Espino, E.; Salazar, R.; Domenek, S.; Ducruet, V. *Ital. J. Food Sci. (Special Issue) SLIM* **2010**, 63.
17. Mattioli, S.; Peltzer, M.; Fortunatia, E.; Armentano, I.; Jimenez, A.; Kenny, J. M. *Carbon* **2013**, *63*, 274.
18. Conn, R. E.; Kolstad, J. J.; Borzelleca, J. F.; Dixler, D. S.; Filer, L. J.; La Du, B. N.; Pariza, M. W. *Food Chem. Toxicol.* **1995**, *33*, 273.
19. Mutsuga, M.; Kawamura, Y.; Tanamoto, K. *Food Addit. Contam. Part A Chem.* **2008**, *25*, 1283.
20. Chemical Compatibility Guide. Thermo Scientific. <http://sevierlab.vet.cornell.edu/resources/Chemical-Resistance-Chart-Detail.pdf> (accessed February 24, **2017**).
21. Barson, C. A.; Dong, Y. M. *Eur. Polym. J.* **1990**, *26*, 4, 449.
22. Standard EN-1186-2002: Migration Testing on Food Contact Materials, **2002**.
23. Commission Regulation (EC) No. 450/2009 on Active and Intelligent Materials and Articles Intended to Come into Contact with Food; Official Journal of the European Union **2009**, L135, pp 3–11.
24. Commission Regulation (EU) No. 10/2011 on Plastic Materials and Articles Intended to Come into Contact with Food; Official Journal of the European Union **2011**, L12, pp 1–89.
25. Arvidsson, B.; Molander, S.; Sanden, B. A. *Hum. Ecol. Risk Assess.* **2013**, *19*, 873.
26. Bhunia, K.; Sablani, S. S.; Tang, J.; Rasco, B. *Compr. Rev. Food Sci. Food Saf.* **2013**, *12*, 523.
27. Kavanagh, N.; Corrigan, O. I. *Int. J. Pharmaceutics* **2004**, *279*, 141.
28. Mitaya, T.; Masuko, T. *Polymer* **1998**, *39*, 5515.
29. Huang, J. Y.; Chieng, Y. Y.; Li, X.; Zhou, W. *Food Bioprocess. Technol.* **2015**, *8*, 382.
30. Rodriguez, E.; Marcos, B.; Huneault, M. *J. Appl. Polym. Sci.* **2016**, *133*, DOI: 10.1002/app.44152
31. Ndazi, B. S.; Karlsson, S. *eXPRESS Polymer Lett.* **2011**, *5*, 119.
32. Miller-Choi, B. A.; Koenig, J. K. *Prog. Polym. Sci.* **2003**, *28*, 1223.
33. De Meulenaer, B. In *Predictive Modeling and Risk Assessment*; Costa, R., Kristbergsson, K., Eds.; Springer, Springer Science + Business Media, LLC, NY, USA, **2009**; Chapter 8, pp 139–154.
34. Ferrara, G.; Bertolodo, M.; Scoponi, M.; Ciardelli, F. *Polym. Degrad. Stab.* **2001**, *73*, 411.
35. Brandsch, J.; Mercea, P.; Ruter, M.; Tosa, V.; Piringer, O. *Food Addit. Contam.* **2002**, *19*, 29.
36. Simoneau, C. JRC Scientific and Technical Reports, *JRC 59476, EUR 24514 EN*, **2010**.
37. Helmroth, I. E.; Dekker, M.; Hamkemeier, A. *J. Appl. Polym. Sci.* **2003**, *90*, 1609.
38. Crank, J. *The Mathematics of Diffusion*, 2nd ed.; Clarendon Press: London, **1975**.
39. Haldimann, M.; Alt, A.; Blanc, A.; Brunner, K.; Sager, F.; Dudler, V. *Food Addit. Contam. Part A* **2013**, *30*, 3, 587.
40. Lyu, S. P.; Untereker, D. *Int. J. Molecular Sci.* **2009**, *10*, 9, 4033.